Polymer Testing 50 (2016) 83–93

Contents lists available at ScienceDirect

Polymer Testing

journal homepage: www.elsevier.com/locate/polytest

Material properties

Effects of the reduction of PAni-coated oxidized multiwall carbon nanotubes on the positive temperature coefficient behaviors of their carbon black/high density polyethylene composites

Seon Hyeong Bae [a], Rama K. Layek [b], Seung Hee Lee [a, b], Tapas Kuila [c], Nam Hoon Kim [b, **], Joong Hee Lee [a, b, *]

[a] Carbon Composite Research Centre, Department of Polymer-Nano Science and Technology, Chonbuk National University, Jeonju, Jeonbuk 54896, Republic of Korea
[b] Advanced Materials Institute of BIN Technology (BK21 plus Global), Dept. of BIN Convergence Technology, Chonbuk National University, Jeonju, Jeonbuk 54896, Republic of Korea
[c] Surface Engineering & Tribology Division, CSIR-Central Mechanical Engineering Research Institute, Council of Scientific & Industrial Research (CSIR), Mahatma Gandhi Avenue, Durgapur 713209, India

ARTICLE INFO

Article history:
Received 30 November 2015
Accepted 5 January 2016
Available online 8 January 2016

Keywords:
Reduction
Polyaniline
Multiwall carbon nanotube
Electrical conductivity
Positive temperature coefficient
Polymer composite

ABSTRACT

Polyaniline (PAni)-coated reduced multiwall carbon nanotubes (PRMWNTs) and carbon black (CB)-filled high-density polyethylene (HDPE) composites (PRMWNTs/CB/HDPE) were prepared through a melt mixing method. Oxidized MWNTs (OMWNTs) were prepared by treating pristine multiwall carbon nanotubes (MWNTs) with an acid mixture (HNO_3:H_2SO_4), and PAni-coated OMWNTs (POMWNTs) were synthesized via in-situ polymerization of aniline monomer in the presence of OMWNTs. POMWNTs were further reduced using hydrazine monohydrate to obtain the PRMWNTs. Fourier transform infrared (FT-IR) spectra and thermogravimetric analysis (TGA) confirmed the formation of PRMWNTs. PRMWNTs showed significantly improved thermal stability and electrical conductivity comparing to POMWNTs. The positive temperature coefficient (PTC) behavior of PRMWNTs/CB/HDPE composites revealed enhanced PTC intensity and electrical conductivity at room temperature compared to POMWNTs/CB/HDPE composites. The PRMWNTs-10/CB/HDPE composite showed high peak resistivity (301.99 MΩ-cm) and low room temperature resistivity compared to the POMWNTs/CB/HDPE composite, and thus showed the highest PTC intensity value of 6.693 as well as very excellent cyclic stability.

1. Introduction

Polymer-based PTC materials are attracting increasing interest because they are flexible, low cost and lightweight materials with good performance [1–6]. PTC materials are employed in various fields such as self-regulating heaters, current protection devices and sensors because of their temperature-activated switching feature [7]. PTC behavior, which indicates a sudden increase in resistivity at the melting temperature (T_m), can be achieved in conducting polymer composites by judicious incorporation of conducting fillers such as CB, carbon nanotubes (CNTs), graphite and metallic particles into an insulating polymer matrix [8–11]. Conducting fillers remain dispersed only in the amorphous region of the polymer and form conducting networks at low temperature. As the temperature approaches the T_m of the polymer, the volume of the polymer expands, and the inter-particle distance become larger, resulting in an increase in resistivity of the composite due to destruction of the conducting networks. Above the T_m, conducting particles in liquid polymer can easily form new conducting networks and thus resistivity decreases. PTC effects can be classified by PTC intensity, PTC behavior, repeatability and room temperature resistivity. To enhance PTC effects, several approaches such as cross-linking of the polymer [12,13], surface treatment and integration of conductive fillers into the insulating polymer [14–18] have been investigated. Among these, integration of conducting fillers of CNTs is one of the most promising routes due to the

* Corresponding author. Carbon Composite Research Centre, Department of BIN Convergence Technology, Chonbuk National University, Jeonju, Jeonbuk 54896, Republic of Korea.
** Corresponding author.
E-mail addresses: nhk@chonbuk.ac.kr (N.H. Kim), jhl@jbnu.ac.kr (J.H. Lee).

http://dx.doi.org/10.1016/j.polymertesting.2016.01.001
0142-9418/

exceptional electrical, mechanical, optical and thermal properties of CNTs [19,20]. In a recent study, HDPE was made by incorporating a conducting MWNTs filler in the HDPE matrix and showed that MWNTs/HDPE composite containing only 5.4 wt.% MWNTs had similar PTC behavior to CB/HDPE composite containing 16 wt.% CB [21]. PTC effects, including PTC intensity and the reproducibility of the CB/HDPE composite, were significantly improved by integration of 0.25 wt% MWNTs [22]. Although MWNTs are excellent fillers for incorporation in polymeric PTC materials, their application is limited by their poor dispersion and nanotube/resin interfacial adhesion induced by strong van der Waals forces and large surface areas [23]. These problems can be solved by introduction of specific functional groups on the surfaces of MWNTs via oxidization and surface modification of the MWNTs. Oxidation of MWNTs occurs via the destruction of the π-conjugated structure of MWNTs, which causes a decrease in electrical conductivity [24]. Functionalization with conducting polymers can increase the compatibility and electrical conductivity of oxidized MWNTs (OMWNTs). Among known conducting polymers, PAni is one of the most promising candidates for fabrication of MWNTs/polymer composites due to its easy synthesis, low cost and excellent environmental stability compared to other conducting polymers [25,26]. Furthermore, PAni doped with dodecyl-benzene-sulfonic acid (DBSA) or camphor sulfonic acid (CSA) shows excellent compatibility with polyolefin composites [27]. PAni coating of MWNTs and CB had a noticeable PTC effect on the resulting HDPE composites compared with unfunctionalized MWNTs-filled composite [28]. By adding PAni to CB/LDPE composites, the percolation threshold was lowered and the composites showed better reproducibility than CB/LDPE composites without PAni [29].

In the present work, MWNTs were oxidized and functionalized with PAni to obtain POMWNTs through an in-situ polymerization technique using various amounts of aniline. Then, POMWNTs were reduced with hydrazine to enhance the electrical conductivity, resulting in PRMWNTs. The resulting POMWNTs and PRMWNTs were used to fabricate POMWNTs/CB/HDPE and PRMWNTs/CB/HDPE composites to investigate effects of the reduction of POMWNTs on the PTC behavior of their composites.

2. Experimental

2.1. Materials

HDPE (2600F, melt flow index = 20 g/10 min) was purchased from Lotte Chemical Co., Korea. CB (particle size ≈ 24 nm, Hi-Black 420B) and multi-wall carbon nanotubes (MWNTs) (CM-95, diameter 10–15 nm, purity > 95%) were obtained from Korea Carbon Black Co. and Hanwha-Nano-tech, Korea, respectively. Dodecyl benzene sulfuric acid (DBSA) was purchased from Tokyo Chemical Industry, Japan, and ammonium persulfate (APS) was purchased from Sigma–Aldrich, USA. Aniline (purity 99%) was obtained from Aldrich and prior to use was purified by vacuum distillation. Sulfuric acid (95%) and nitric acid (60%) were received from Samchun Pure Chemical Co. Ltd, Korea. Hydrazine hydrates (Sigma Aldrich, USA) and xylene (Samchun Pure Chemical Co. Ltd, Korea) were used as-received.

2.2. Oxidation of MWNTs

Pristine MWNTs were poured into a concentrated sulfuric and nitric acid (3:1) mixture to obtain OMWNTs. The mixture was sonicated for 20 min and then refluxed at 110 °C for 1 h. The OMWNTs were washed with DI-water until the pH value reached around ~7.0, and then filtered. Finally, OMWNTs were obtained by drying the obtained black mass in a vacuum oven at 60 °C for 24 h.

2.3. Synthesis of POMWNTs by in-situ polymerization

POMWNTs were synthesized by in-situ polymerization of aniline monomer in the presence of OMWNTs. Typically, 0.1 g of OMWNTs was dispersed in 150 mL of a 0.1 (M) aqueous solution of DBSA via ultrasonication (30 min). Then, the desired amount of aniline monomer was added with constant stirring. An aqueous solution of APS (same molality as the aniline monomer) was added drop-wise into the reaction mixture at constant stirring to initiate the polymerization of aniline. The reaction mixture was stirred for an additional 6 h at room temperature. A dark green suspension, which indicated the formation of the emeraldine salt, was observed. The obtained product was washed with acetone and DI water several times to remove impurities such as unreacted monomer, excess DBSA, oxidant and oligomers. Finally, the POMWNTs were collected by drying in a vacuum oven at 60 °C for 24 h. The same procedure was used to synthesize different POMWNTs by varying the weight ratios of OMWNTs and aniline. The weight ratios of OMWNTs and monomer aniline used to prepare POMWNTs were 90: 10, 80: 20, and 70: 30, and the resulting products were designated POMWNTs-10, POMWNTs-20, and POMWNTs-30, respectively. For comparison, pure PAni was synthesized using the same procedure without OMWNTs.

2.4. Preparation of PRMWNTs

Chemical reduction of POMWNTs using hydrazine monohydrate was carried out to obtain PRMWNTs. POMWNTs (0.1 g) were dispersed in 50 ml of DI-water by ultrasonication for 30 min. Then, the mixture was treated with 0.1 mL hydrazine monohydrate at 95 °C for 12 h. The obtained product was filtered and repeatedly washed with DI water to remove excess hydrazine hydrate. Finally, PRMWNTs were collected by drying in a vacuum oven at 60 °C for 24 h Scheme 1 shows the processes used to synthesize POMWNTs and PRMWNTs.

2.5. Preparation of composites

Master batches were prepared by solution mixing the HDPE and PRMWNTs in xylene at 110 °C for 30 min. The resulting PRMWNTs/HDPE master batch was melt-mixed with additional HDPE and CB particles in a Haake mixer (Rheocord 9000, Germany) at 180 °C for 30 min to obtain PRMWNTs/CB/HDPE composites. Specimens with a diameter of 10 mm and thickness of 1.2 mm were prepared by compression-molding at 180 °C under constant pressure for 5 min using a hot press The POMWNTs/CB/HDPE composites were fabricated using the same procedure. The HDPE and CB composite was also melt-mixed in a Haake mixer at 180 °C for 30 min and molded by compression molding as described above.

2.6. Characterization

The morphologies of composites were examined using field emission scanning electron microscopy (FE-SEM) (JSM-670F, JEOL, Japan) in Jeonju Center of KBSI and high-resolution transmission electron microscopy (FETEM) (FEI Titan G2 60–300, USA, operated at 80 kV). Fourier transform infrared (FT-IR) spectra were recorded using a JASCO FTIR-300E spectrometer (Japan) in the wave number range of 4000–500 cm^{-1}. Samples were prepared by grinding them with KBr and making pellets by the compression method. Pure KBr was used as a reference. Thermogravimetric analysis of samples

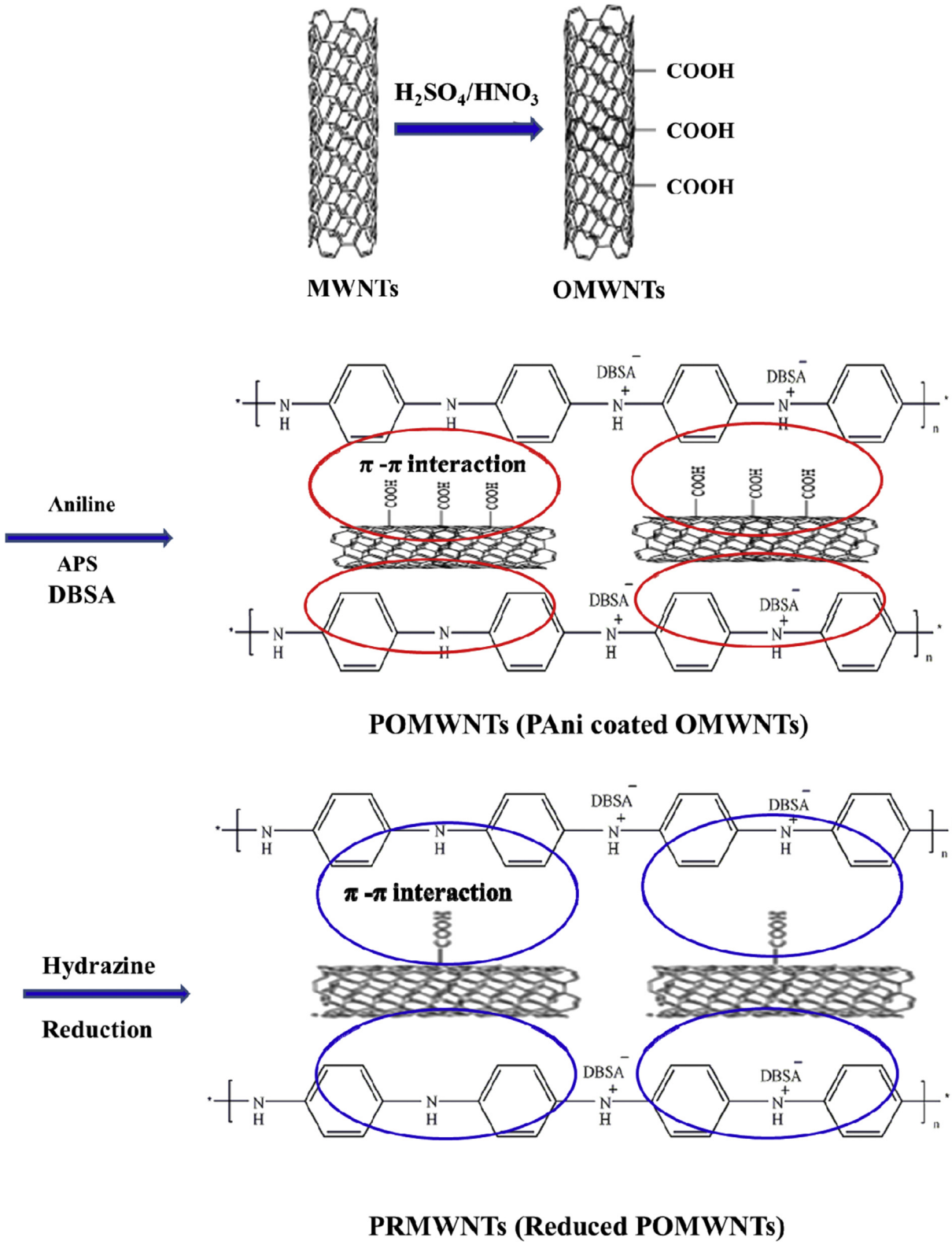

Scheme 1. Schematic of the synthesis processes for POMWNTs and PRMWNTs.

(TGA) was performed using a TGA Q50 (TA instrument, USA) within the temperature range of 30–800 °C at a heating rate of 10 °C/min under a nitrogen atmosphere. Electrical conductivity was measured using a programmable DC voltage/current detector at a constant voltage of 10 mV. The resistivity of each sample was obtained from a four-point probe instrument using the following equations:

$$\text{Resistivity } (\rho)(\Omega - cm) = \pi t / \ln 2 (V/I) = 4.53 \times t \times (resistance)$$

$$\text{Conductivity}(\sigma)(S/cm) = 1/\rho$$

where t is the thickness of the sample, V is the measured voltage and I is the source current. Volume resistivity (ρ) was measured as a function of temperature using a computerized measurement system comprising a programmable oven and Keithley 2000 (USA). The sample was heated at a rate of 2 °C/min from room temperature to 190 °C. Prior to resistivity measurements, both sides of the sample surfaces were coated with silver paste to ensure good contact between the sample and electrode.

Differential scanning calorimetry (DSC) was performed using a Q40 system (TA Instruments, USA) with a heating rate of 10 °C/min from ambient temperature to 170 °C under nitrogen flow. Linear thermal expansion of composites was measured using TMA Q400 (TA Instruments, USA) under a nitrogen atmosphere. Specimens with dimensions of 0.5 × 0.5 × 0.1 cm were prepared and experiments were performed at a heating rate of 2 °C/min in the temperature ranging from 40 to 190 °C. The coefficient of thermal expansion (CTE) value was calculated from;

$$CTE = \frac{L_s}{L_o \times \Delta T}$$

here, L_s is the changed length, L_o is the initial length of the prepared sample, and ΔT is the change in temperature.

3. Results and discussion

3.1. FT-IR analysis

To characterize and analyze the functional groups in pure PAni, raw MWNTs, OMWNTs, reduced OMWNTs (RMWNTs), POMWNTs, and PRMWNTs, FT-IR measurements were carried out, and the resulting spectra are presented in Fig. 1(a) and (b). The FT-IR spectrum of raw MWNTs exhibited absorption bands at 3446 cm^{-1} due to OH stretching in carboxylic acid, 2858 and 2925 cm^{-1} due to asymmetric and symmetric stretching of CH_2, and 1633 cm^{-1} due to conjugated C=C stretching [30]. This result signified that some functional groups were already present on the surfaces of the raw MWNTs. OMWNTs exhibited new absorption bands at 1710 cm^{-1} corresponding to C=O stretching vibrations and 1168 cm^{-1} due to the stretching vibration of the C–O bond of carboxylic acid (–COOH) [31]. In addition, the OMWNT spectrum showed a characteristic band at 1396 cm^{-1} due to the –OH bending deformation present in COOH [32]. All observations clearly indicated the successful formation of OMWNTs via oxidation of raw MWNTs. The FT-IR spectrum of POMWNTs was characterized by absorption bands at 1558 and 1490 cm^{-1} associated with N = Q = N stretching (quinoid band) and N–C–N stretching (benzenoid band), respectively. The absorption peaks at 1295 and 1240 cm^{-1} were attributed to C–N (–N-benzenoid-N-) and –N = quinoid = N–, respectively. In addition, the band at 1122 cm^{-1} was attributed to sulfonic group (S=O) stretching vibrations (arising from the dopant BDSA), and the band at 795 cm^{-1} to aromatic C–H out-of-plane bending vibrations [33]. From the FT-IR spectra, it was obvious that PAni was successfully anchored on the surface of the OMWNTs. In RMWNTs, the peak intensity of the –COOH group (1710 cm^{-1}) decreased, but was still present. This indicated that hydrazine monohydrate was not able to fully remove oxygen functional groups. PRMWNTs showed both the characteristic peaks of RMWNTs and PAni. As the PAni content increased, so did the intensity of the characteristic peaks of PAni in both POMWNTs and PRMWNTs specimens.

3.2. TGA analysis

To determine the amount of functional groups present in OMWNTs, POMWNTs, and PRMWNTs, thermogravimetric analysis (TGA) of PAni, raw MWNTs, OMWNTs, POMWNTs, and PRMWNTs was carried out. The results are presented in Fig. 2(a) and (b). The TGA thermogram of raw MWNTs showed minor weight loss up to 500 °C. Weight loss of ~7.7% was observed within the temperature range of 500–800 °C, which was attributed to amorphous carbon impurities [34]. A continuous weight decrease of 18.3% up to 800 °C was observed due to the removal of oxygen-containing functional groups and amorphous carbon. However, the RMWNTs showed less weight decrease of 13.5% than OMWNTs due to the removed functional groups. In contrast, PAni and POMWNTs showed three weight loss steps. The first weight loss was observed at ~100 °C due to the removal of water molecules. The second weight loss was observed in the temperature range of 250–500 °C due to the loss of low molecular weight polymers, oligomers and unbounded dopant (DBSA). The final weight loss occurred in the temperature range of 500–800 °C due to degradation of the backbone of PAni and OMWNTs [21,35]. The amount of anchored PAni on the surface of OMWNTs was calculated from the weight loss and is reported in Table 1. The amounts of PAni in POMWNTs increased as the aniline

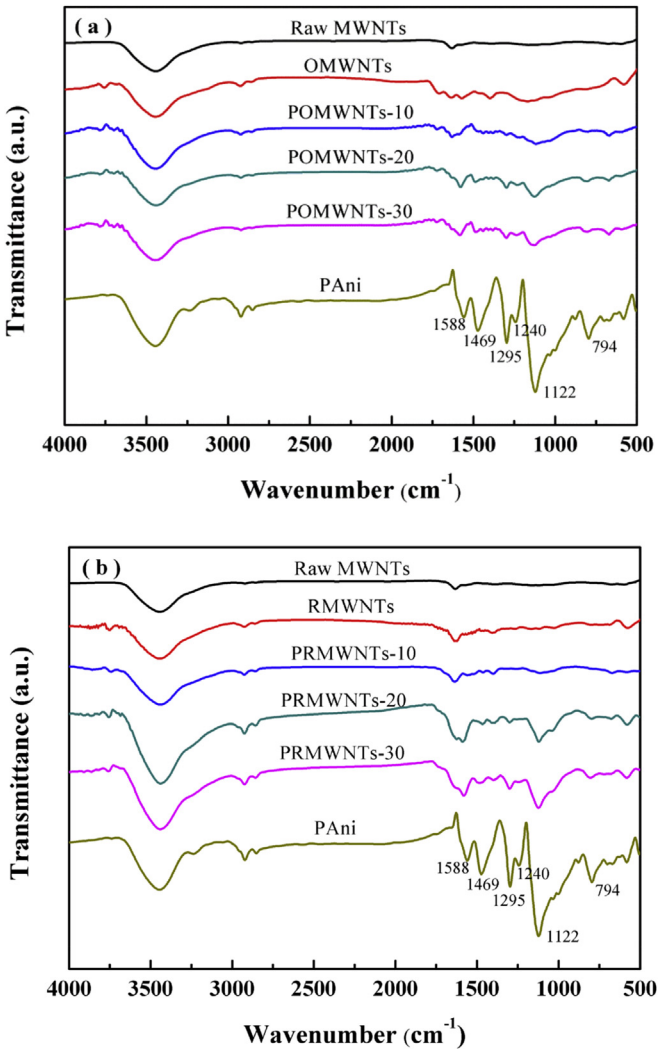

Fig. 1. FT-IR spectra of various (a) POMWNTs and (b) PRMWNTs.

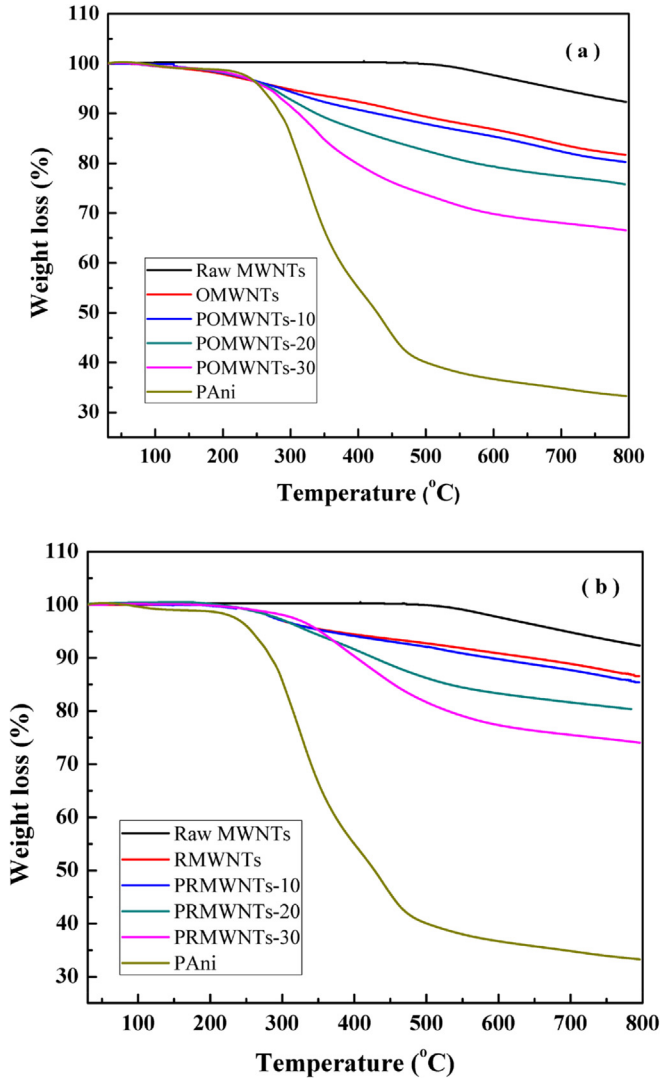

Fig. 2. TGA curves for various (a) POMWNTs and (b) PRMWNTs.

monomer content increased. The amounts of PAni were ranged from 7.1 to 38.5 wt%. The onset degradation temperature of PRMWNTs was shifted to a higher temperature than that of POMWNTs, and PRMWNTs had significantly better thermal stability than POMWNTs. This was due to the disappearance of the majority of oxygen-containing functional groups in PRMWNTs.

3.3. Electrical conductivity

Electrical conductivities of PAni, OMWNTs, and various POMWNTs and PRMWNTs were measured using a four-point instrument. Results are presented in the form of a bar diagram in Fig. 3. OMWNTs exhibited the highest conductivity of 16.16 S/cm, whereas PAni had a low conductivity of 0.26 S/cm. The conductivity

Table 1
PAni contents in POMWNTs determined by TGA.

Sample	PAni content (wt. %)
OMWNTs	–
POMWNTs-10	7.1
POMWNTs-20	16.8
POMWNTs-30	38.5

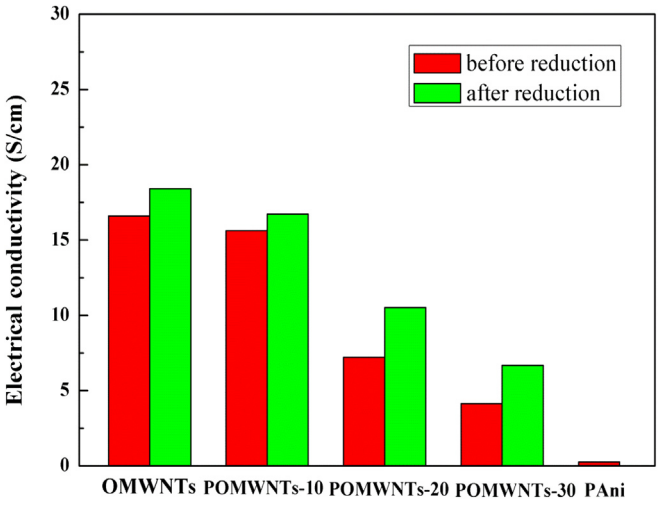

Fig. 3. Electrical conductivities of PAni, OMWNTs, and various contents of POMWNTs before and after reduction.

of POMWNTs decreased continuously with increasing the PAni content. This result indicated that the amount of PAni coated on the MWNT surface affected conductivity. However, the conductivity of POMWNTs was still higher than that of pure PAni. After reduction, the PRMWNTs exhibited a significant increment in conductivity due to the removal of insulating oxygen functionalities on the surface.

HDPE composites with 5, 10, 15 and 25 wt.% CB were prepared and their room temperature resistivity measured. Log room temperature resistivities are presented in Fig. 4. A dramatic drop in resistivity of the composites was observed up to 15 wt.% CB. This phenomenon is normally attributed to the percolation threshold at which more conducting channels are formed. PTC materials normally require filler content above this percolation threshold. As the CB content approached 15 wt.%, more conducting channels started to form and, therefore, a sharp drop in resistivity was observed from 1.96 MΩ-cm at 10 wt.% to 119.81 Ω-cm at 15 wt.%. These results indicated that 15 wt.% CB loading was optimum to fabricate CB/HDPE composite-based PTC materials. CB/HDPE (15/85) composites with various POMWNTs and PRMWNTs contents were

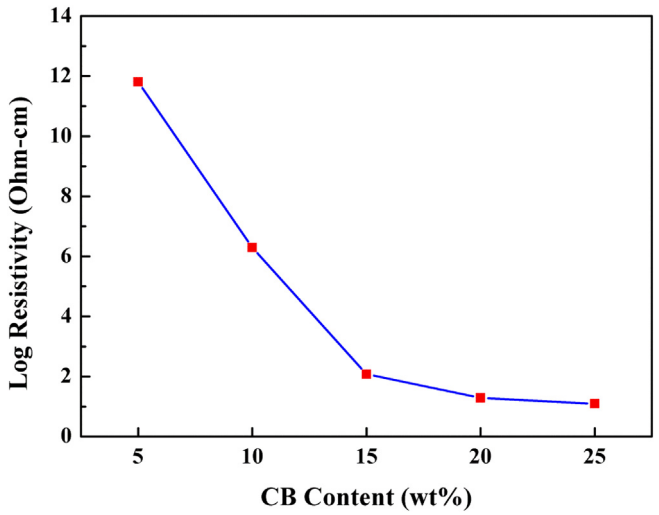

Fig. 4. Log room temperature resistivity of CB/HDPE composite with various CB contents.

fabricated to investigate the effects of each component on the PTC behavior of the composites.

3.4. PTC behavior

Log resistivity curves of OMWNTs/CB/HDPE (CB/HDPE = 15/85) composites with different contents of OMWNTs at various temperatures are shown in Fig. 5. It is clear that OMWNTs/CB/HDPE composites showed only slight changes in resistivity up to 100 °C with increasing temperature, but a rapid increase above 115 °C. As the content of OMWNTs increased, room temperature resistivity decreased from 114.82 to 64.56 Ω-cm due to the formation of better conductive channels by bridging of CB fillers with OMWNTs. However, the maximum PTC intensity (I_{PTC}) value of 5.81 was observed at 0.25 wt.% OMWNTs loading in CB/HDPE (15/85) composites. This indicated that a further increase in OMWNTs content in CB/HDPE composites lowered I_{PTC} due to the presence of unbroken conducting channels during volume expansion [17,18]. Hence, the CB/HDPE composite with 0.25 wt.% OMWNTs was chosen for further investigation.

POMWNTs/CB/HDPE and PRMWNTs/CB/HDPE composites (weight ratios of 0.25/15/85) were fabricated and their PTC behavior with temperature are shown in Fig. 6(a) and (b). Similarly, the same amounts of OMWNTs (0.25 wt.%), POMWNTs-10, POMWNTs-20, POMWNTs-30, RMWNTs (0.25 wt%), PRMWNTs-10, PRMWNTs-20 and PRMWNTs-30 were introduced into CB/HDPE (15/85) composites. The room temperature resistivity of POMWNTs-10/CB/HDPE was much lower than those of CB/HDPE and OMWNTs/CB/HDPE composites. This may be due to the promoting the formation of conducting channels of PAni in the OMWNTs network. However, for POMWNTs-20/CB/HDPE and POMWNTs-30/CB/HDPE composites, the room temperature resistivity increased with increasing the PAni content. This may be due to an increase in thickness of the PAni coating layer on POMWNTs. PRMWNTs-20/CB/HDPE composite showed the lowest resistivity among the composites tested. To investigate the PTC behavior of POMWNTs/CB/HDPE and PRMWNTs/CB/HDPE composites, the resistivity of composites was measured at various temperatures. The log resistivity curves with temperature are shown in Fig. 6 and summarized in Table 2. All composites showed very similar trends in PTC behavior with temperature to the OMWNTs/CB/HDPE composite (Fig. 5). The PTC intensity (I_{PTC}) of the composites ranged from 4.969 to 6.693 (Table 2). PRMWNTs/CB/HDPE composites had lower room resistivity and higher PTC intensities than the POMWNTs/CB/HDPE composites with the same amount of filler. PAni coating of OMWNTs decreased the surface free energy of OMWNTs, which promoted better interaction between the filler and HDPE [29]. Some conducting paths in the composites would probably be broken during the

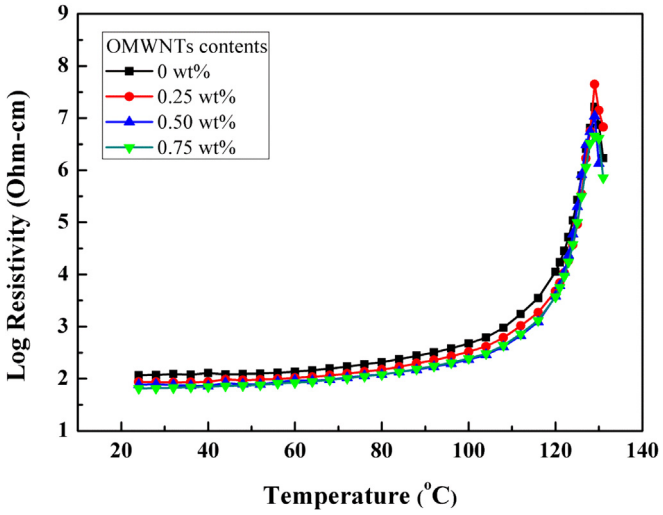

Fig. 5. Log resistivities of OMWNTs/CB/HDPE composites with different contents of OMWNTs at various temperatures.

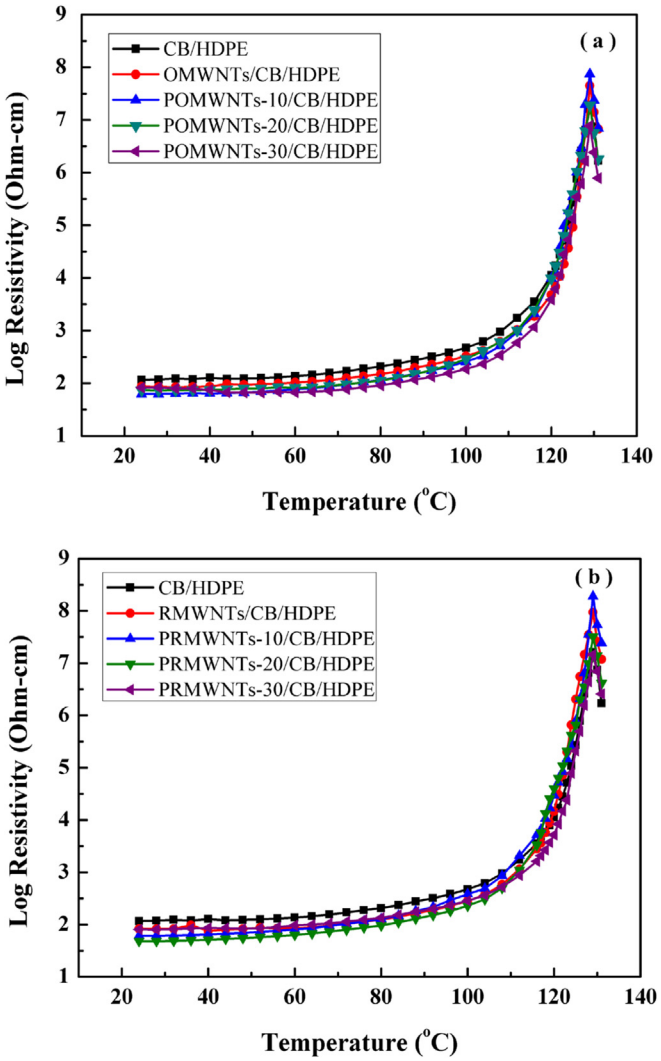

Fig. 6. Log resistivity of various (a) POMWNTs/CB/HDPE and (b) PRMWNTs/CB/HDPE composites.

Table 2
Resistivity and PTC intensities of the composites.

Type of fillers added into CB/HDPE	ρ_{RT}[a]	ρ_{max}[b] ($\times 10^6$)	I_{PTC}[c]
–	199.95	12.94	5.033
OMWNTs	87.70	56.10	5.806
POMWNTs-10	62.66	122.18	6.290
POMWNTs-20	73.96	30.13	5.610
POMWNTs-30	83.37	7.76	4.969
RMWNTs	82.60	118.57	6.157
PRMWNTs-10	61.23	301.99	6.693
PRMWNTs-20	47.86	63.68	6.124
PRMWNTs-30	80.35	18.40	5.360

[a] Room temperature resistivity.
[b] Maximum resistivity.
[c] PTC intensity as the ratio of log (ρ_{max}/ρ_{RT}).

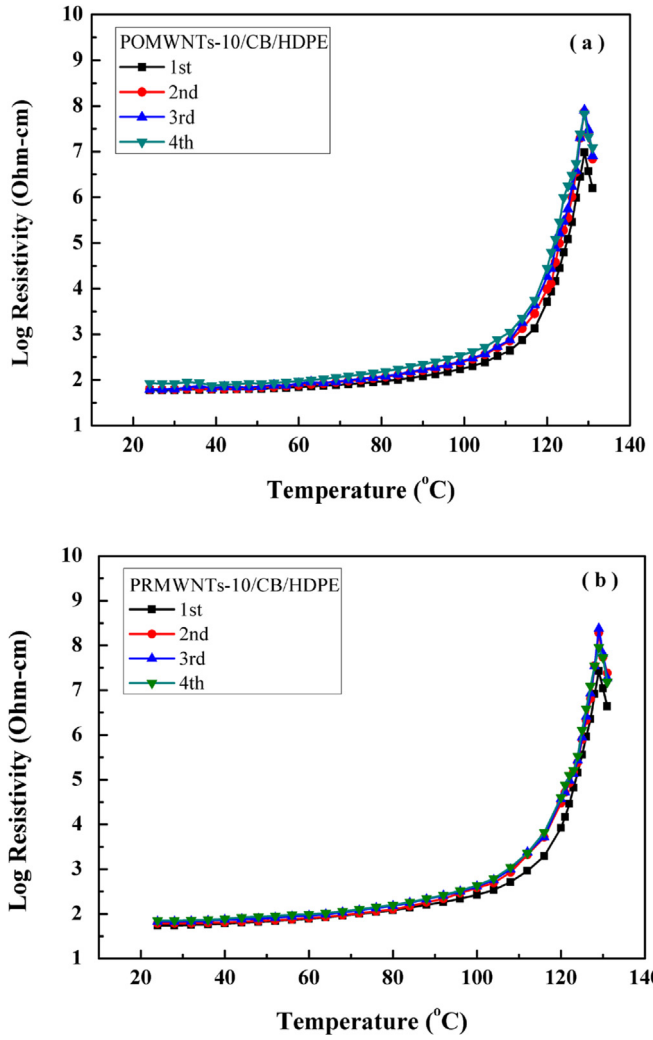

Fig. 7. PTC behaviors of (a) POMWNTs-10/CB/HDPE and (b) PRMWNTs-10/CB/HDPE for repeated 4 heating and cooling cycles test.

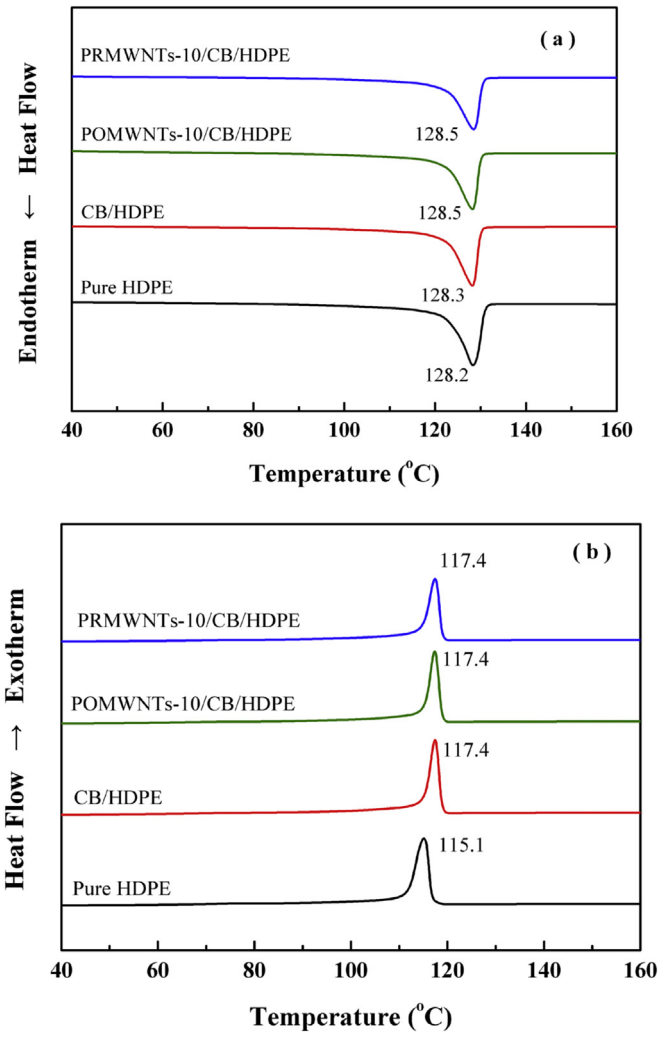

Fig. 8. DSC thermograms for (a) heating and (b) cooling cycles of HDPE and its composites.

expansion of the polymer, which makes longer distances between conducting particles. An increase of the amount of PAni helped to prolong forming the conducting networks between fillers at high temperature due to the presence of the conducting media around fillers. Thus, it causes higher peak resistivity with increasing the amount of PAni. Hydrazine treatment of POMWNTs restored the π-conjugated structure, resulting in the activation of the surface-free energy of PRMWNTs, and thus an increase in PTC performance. The PRMWNTs/CB/HDPE composites showed higher I_{PTC} values than POMWNTs/CB/HDPE composites. Among POMWNTs composites, POMWNTs-10 composite exhibited the highest I_{PTC} value of 6.290. Same as POMWNTs-10 composite, PRMWNTs-10/CB/HDPE composite also showed the highest I_{PTC} value of 6.693.

The cyclic stability of the composites was also monitored for POMWNT-10/CB/HDPE and PRMWNT-10/CB/HDPE composites through four repeated heating and cooling cycle tests, as shown in Fig. 7. For both composites, a slight change after the first cycle was observed. Almost constant room temperature resistivity was observed, but the peak resistivity became a little higher after the first cycle due to the stabilized structures of the composites. From the second cycle, the PTC curves of PRMWNT-10/CB/HDPE composite showed very similar behaviors, indicating that the composite had an excellent repeatability. This phenomenon might be due to stabilization of the HDPE crystalline structures in the composites by heat treatment and annealing [36,37], which was confirmed by the DSC results (Fig. 8).

3.5. DSC analysis

DSC study of the composites was performed to study the effects of the fillers on thermal behavior and to analyze PTC behaviors of the composites. The DSC results obtained for pure HDPE and its composites are shown in Fig 8. Pure HDPE and composites films had almost the same meting temperature, indicating that the T_m is not affected by the addition of fillers. However, the crystallization temperature (T_c) of the composites was shifted to a temperature slightly higher (2 °C) than that of pure HDPE. This indicated that crystallization of HDPE was hampered by the presence of fillers [34]. DSC thermograms of POMWNTs-10/CB/HDPE and PRMWNTs-10/CB/HDPE composites were also measured for 4 repeated heating cycles as shown in Fig. 9 (a) and (b), respectively. The T_m of both composites in the 2nd heating cycle was shifted to a lower temperature than that obtained after the 1st heating cycle, indicating a decrease in crystal size and destruction of the pseudo-transition behavior of HDPE. For 2nd–4th heating cycles, both composites

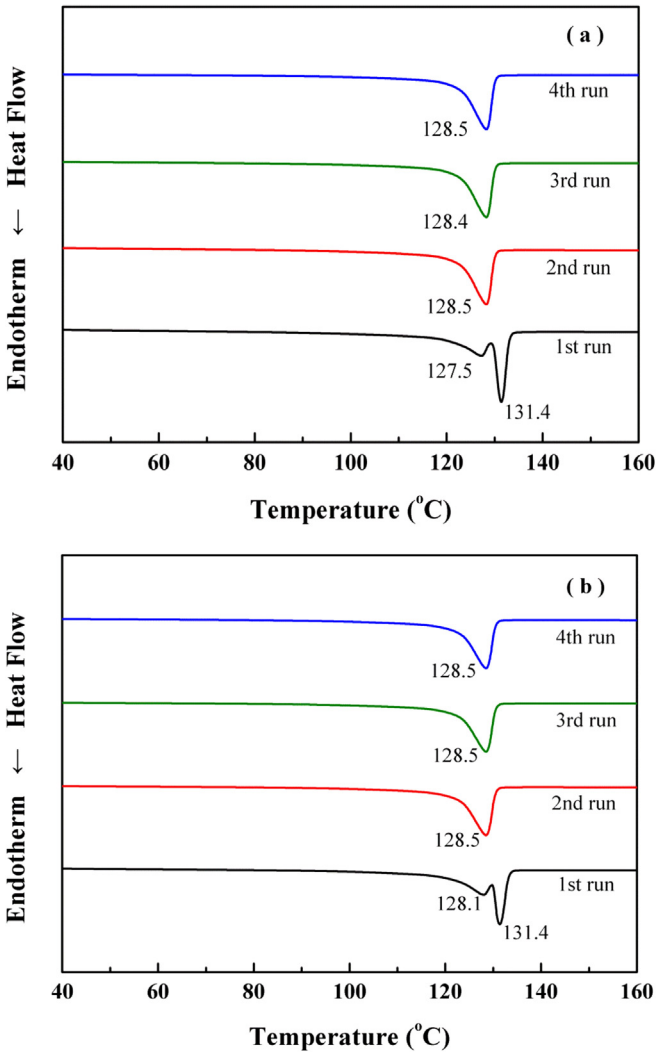

Fig. 9. DSC thermograms for (a) POMWNTs-10/CB/HDPE and (b) PRMWNTs-10/CB/HDPE composites for repeated 4 heating cycles.

show the same T_m, indicating stabilization of the crystalline phase of the composites. This explained the good PTC repeatability of the melt characteristics of the composites after the 1st heating cycle. This type of phenomenon has been also reported in low molecular weight polyethylene/ultra-high molecular weight polyethylene blends [38,39]. The DSC results for HDPE and its composites according to the number of heating and cooling cycles are summarized in Tables 3 and 4. Pure HDPE had the crystallinity (X_c) of 68.3% and enthalpy (ΔH_m) of 167.5 J/g; while in the CB/HDPE composites, these values decreased to 64.56% and 134.6 J/g, respectively, calculated from DSC curves for the 2nd heating cycle. This may be due to the change in the crystal size of HDPE in the presence of CB particles. The X_c and ΔH_m of POMWNTs-10/CB/HDPE and PRMWNTs-10/CB/HDPE composites were higher than those of the CB/HDPE composites. The highest X_c and ΔH_m values were 67.48% and 145 J/g for PRMWNTs-10/CB/HDPE.

3.6. Morphology

HRTEM and FE-SEM characterizations of CB/HDPE and PRMWNTs-10/CB/HDPE were carried out and results were presented in Figs. 10 and 11. The CB particles shown in Fig. 10(a) were slightly aggregated in the HDPE matrix. However, during melt mixing, the viscous HDPE chains enter between the agglomerated CB particles, enabling separation of the agglomerated CB particles. PRMWNTs-10/CB/HDPE composite showed better dispersion in the HDPE matrix than CB/HDPE composite due to the better dispersion of PAni coated particles, as shown in Fig. 10 (b). The morphologies of the fractured surfaces of CB/HDPE and the PRMWNTs-10/CB/HDPE composite are significantly different, as shown in Fig. 11(a) and (b). PRMWNTs-10/CB/HDPE composite had a rougher surface than CB/HDPE due to better dispersion of fillers and the presence of MWNTs with high aspect ratio.

3.7. Thermal expansion

The coefficients of thermal expansion (CTE) of pure HDPE and its composites were measured by TMA and results are presented in Fig. 12. A sudden change in thermal expansion was observed in the T_m region of HDPE (temperature range of around 131–133 °C) due to a sudden decrease in viscosity of the polymer, which caused an increase in segmental motion of the polymer chain in the melt state. Furthermore, the CTE values of the composites were lower than those of pure HDPE. Relatively low CTE filler values compared with those of HDPE indicated that the filler acted as a barrier to thermal expansion of the polymer composites. We also noted that the PRMWNTs-10/CB/HDPE composite had a higher CTE value than POMWNTs-10/CB/HDPE. This phenomenon can be explained by better activation of the segmental motion of HDPE chains by phonon mode vibration and Brownian motion of the PRMWNTs compared to POMWNTs [40]. It is well established that PTC behavior is related to the thermal expansion of the polymer used in the composite [41–43], but we found a difference between the PTC behavior and thermal expansion. CTE values increased continuously as the temperature increased, whereas the resistivity of the composites did not show any remarkable change up to 100 °C, but rather a sudden increase around the melting temperature. As the inter-particle distance in the composite increased continuously due to thermal expansion, electron transfer was hampered. FESEM analysis of CB/HDPE and the PRMWNTs-10/CB/HDPE composite provided an insight into filler distribution and demonstrated the existence of small voids in the HDPE matrix. The voids between HDPE and fillers may have been caused by incomplete adhesion, and thus increased the resistivity and instability of the PTC materials. These voids would have been

Table 3
Melt characteristics of HDPE and its composites obtained by DSC for 4 heating cycles.

Sample	First scan		Second scan		Third scan		Fourth scan		Crystallinity (X_c) (%)
	T_m (°C)	ΔH_m (J/g)	T_m (°C)	ΔH_m (J/g)	T_m (°C)	ΔH_m (J/g)	T_m (°C)	ΔH_m (J/g)	
HDPE	128.5	147.1	128.3	167.5	128.3	165.5	128.3	166.1	68.30
CB/HDPE	128.5 131.7	146.5	128.5	134.6	128.3	134.5	128.2	135.0	64.56
POMWNTs-10/CB/HDPE	127.8 131.4	147.1	128.5	137.6	128.3	138.7	128.2	138.8	65.99
PRMWNTs-10/CB/HDPE/	128.1 131.4	146.0	128.5	140.7	128.5	140.2	128.5	141.1	67.48

Crystallinity was calculated from the ratio of the measured ΔH_m(second scan) of the composites to ΔH_{m0} of 100% crystalline polyethylene (245.3 J/g) [14].

Table 4
Melt characteristics of HDPE and its composites obtained by DSC for 4 cooling cycles.

Sample	First scan		Second scan		Third scan		Fourth scan	
	T_c (°C)	ΔH_c(J/g)	T_c (°C)	ΔH_c(J/g)	T_c (°C)	ΔH_c(J/g)	T_c (°C)	ΔH_c(J/g)
HDPE	115.2	161.9	115.1	165.0	115.1	165.7	115.1	166.3
CB/HDPE	117.4	139.1	117.4	141.2	117.4	141.3	117.5	141.0
POMWNTs-10/CB/HDPE	117.3	142.4	117.4	143.4	117.4	143.0	117.4	143.7
PRMWNTs-10/CB/HDPE	117.3	144.4	117.4	145.8	117.4	145.3	117.4	145.0

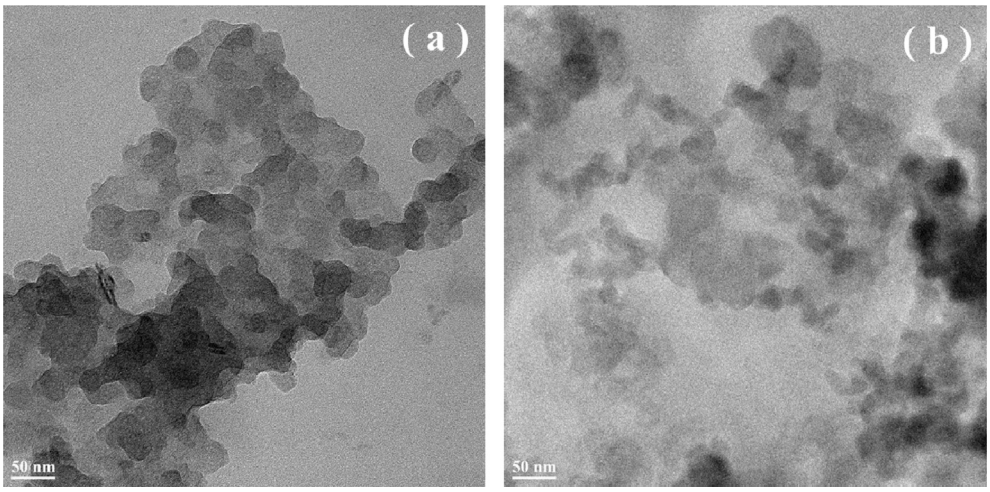

Fig. 10. HRTEM images of (a) CB/HDPE and (b) PRMWNT-10/CB/HDPE composites.

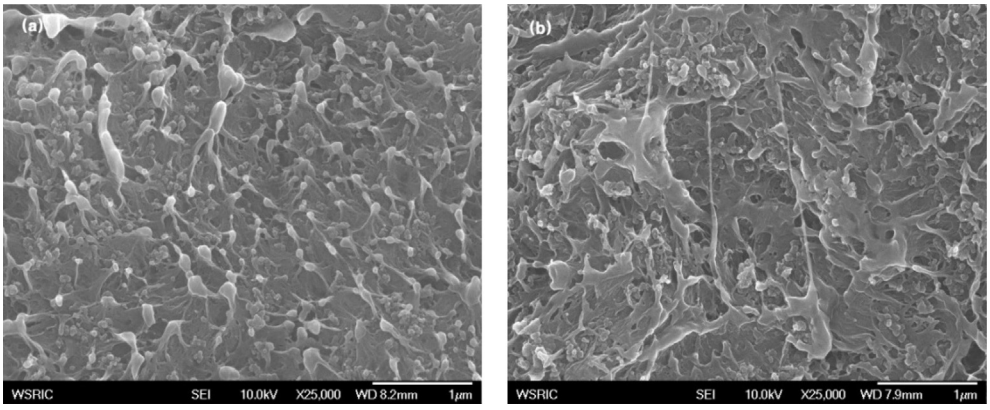

Fig. 11. FE-SEM images of (a) CB/HDPE and (b) PRMWNT-10/CB/HDPE composites.

expanded with increasing temperature and resulted in composites with different CTE values, leading to fluctuation in PTC behavior [44,45]. Above the melting temperature, the sudden decreases in CTE values of samples were observed, and thus caused the sudden decease in resistivity.

4. Conclusions

OMWNTs were prepared by oxidizing pristine MWNTs with an acid mixture (HNO_3:H_2SO_4). POMWNTs were prepared by in-situ polymerization of PAni in the presence of OMWNTs by varying the weight ratio of OMWNTs and PAni. POMWNTs was reduced by treating hydrazine hydrate to obtain PRMWNTs. FT-IR and TGA results confirmed the successful formation of OMWNTs, POMWNTs, and PRMWNTs. TGA thermograms of POMWNTs and PRMWNTs confirmed the amount of PAni coated on the surface. The electrical conductivity of PRMWNTs was higher than that of POMWNTs. The X_c and ΔH_m values of the PRMWNTs/CB/HDPE composites in DSC analysis were higher than those of the POMWNTs/CB/HDPE and CB/HDPE composites. The PRMWNTs-10/CB/HDPE composite had a higher CTE value than POMWNTs-10/CB/HDPE composite. The reduced PRMWNTs/CB/HDPE composites showed lower room temperature resistivity and higher PTC intensity than POMWNTs/CB/HDPE composites. PRMWNTs-10/CB/HDPE composite also showed the highest PTC intensity of 6.693 as well as very excellent repeatability.

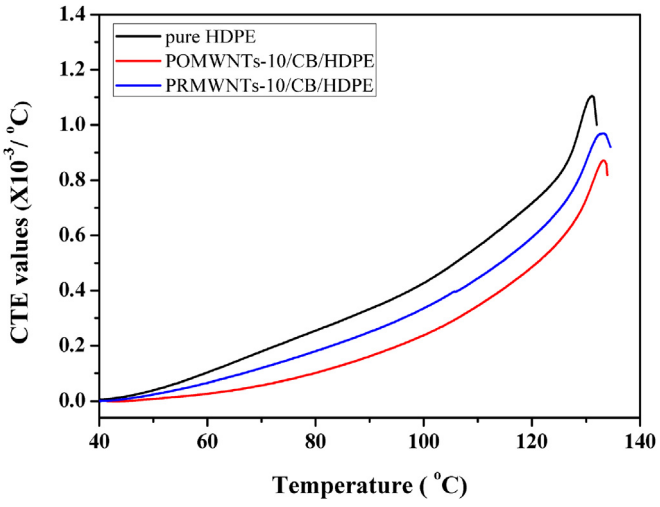

Fig. 12. CTE values of pure HDPE and its composites at various temperatures.

Acknowledgments

This study was supported by the Basic Research program (2014R1A1A2056213) and the Basic Research Laboratory Program (2014R1A4A1008140) through the Korea Research Foundation (KRF) from the Ministry of Science, ICT & Future Planning of Korea.

References

[1] Q. Li, B. Siddaramaiah, N.H. Kim, S.B. Heo, J.H. Lee, Synergy effect of hybrid fillers on the positive temperature coefficient behavior of polypropylene/ultra-high molecular weight polyethylene composites, J. Appl. Polym. Sci. 116 (2010) 116.
[2] Y. Zeng, G. Lu, H. Wang, J.H. Du, Z. Ying, C. Liu, Positive temperature coefficient thermistors based on carbon nanotube/polymer composites, Sci. Rep. UK 4 (2014) 6684.
[3] Y. Qu, W. Zhang, K. Dai, G. Zheng, C. Liu, J. Chen, C. Shen, Tuning of the PTC and NTC effects of conductive CB/PA6/HDPE composite utilizing an electrically superfine electrospun network, Mater. Lett. 132 (2014) 48.
[4] C. Lu, R. Wang, X.N. Hu, Q.Q. Cao, X.H. Huang, Y.X. He, Y.Q. Zhang, Influence of morphology on PTC effect for poly (ethylene-co-butyl acrylate)/nylon6 blends with multiwall carbon nanotubes dispersed at interface and in matrix, Polym. Bull. 71 (3) (2014) 545.
[5] R. Zhang, P. Tang, J. Li, D. Xu, Y. Bin, Study on filler content dependence of the onset of positive temperature coefficient (PTC) effect of electrical resistivity for UHMWPE/LDPE/CF composites based on their DC and AC electrical behaviors, Polymer 55 (8) (2014) 2103.
[6] G. Yu, M.Q. Zhang, H.M. Zeng, Y.H. Hou, H.B. Zhang, Effect of filler treatment on temperature dependence of resistivity of carbon-black-filled polymer blends, J. Appl. Polym. Sci. 73 (1999) 489.
[7] J.H. Kim, H.N. Cho, S.H. Kim, J.Y. Kim, PTC behavior of polymer composites containing ionomers upon electron beam irradiation, Macromol. Res. 12 (2004) 53.
[8] E. Frydman, Improvement in or relating to resistance elements having positive temperature/resistance characteristic, U. K. Pat. 604–695 (1948).
[9] F. Kohler, Resistance element, U. S. Pat. 3243753 (1966).
[10] J. Meyer, Glass transition temperature as a guide to selection of polymers suitable for PTC materials, Polym. Eng. Sci. 13 (1973) 462.
[11] K. Ohe, Y. Naito, New resistor having an anomalously large positive temperature coefficient, J. Appl. Phys. 10 (1971) 99.
[12] W. Jia, X. Chen, S. Li, Effects of irradiation on PTC performance of LDPE/EPDM blends filled with carbon blacks, J. Appl. Polym. Sci. 60 (1996) 2317.
[13] M. Narkis, A. Vaxman, Resistivity behavior of filled electrically conductive cross-linked polyethylene, J. Appl. Polym. Sci. 29 (1984) 1639.
[14] J.F. Zhang, Q. Zheng, Y.Q. Yang, X.S. Yi, High-density polyethylene/carbon black conductive composites I; effect of CB surface modification on its resistivity-temperature behavior, J. Appl. Polym. Sci. 83 (2002) 3112.
[15] G. Yu, M.Q. Zhang, H.M. Zeng, Carbon-black-filled polyolefine as a positive temperature coefficient material: effect of composition, processing, and filler treatment, J. Appl. Polym. Sci. 70 (1998) 559.
[16] H. Pang, Y.C. Zhang, T. Chen, B.Q. Zeng, Z.M. Li, Tunable positive temperature coefficient of resistivity in an electrically conducting polymer/graphene composite, Appl. Phys. Lett. 96 (2005) 251907.
[17] J.F. Gao, D.X Yan, H.D. Huang, K. Dai, Z.M. Li, Positive temperature coefficient and time-dependent resistivity of carbon nanotubes (CNTs)/ultrahigh molecular weight polyethylene (UHMWPE) composite, J. Appl. Polym. Sci. 114 (2009) 1002.
[18] Q. Li, B. Siddaramaiah, N.H. Kim, G.H. Yoo, J.H. Lee, Positive temperature coefficient characteristic and structure of graphite nanofibers reinforced high density polyethylene/carbon black nanocomposite, Compos. Part B Eng 40 (2009) 218.
[19] K.T. Lau, D. Hui, The revolutionary creation of new advanced materials-carbon nanotube composites, Compos. Part B Eng 33 (2002) 263.
[20] X.L. Xie, Y.W. Maia, X.P. Zhou, Dispersion and alignment of carbon nanotubes in polymer matrix: a review, Mater. Sci. Eng. R 49 (2005) 89.
[21] X.J. He, J.H. Du, Z. Ying, H.M. Cheng, Positive temperature coefficient effect in multiwalled carbon nanotubes/high density polyethylene composites, Appl. Phys. Lett. 86 (2005) 062112.
[22] J.H. Lee, S.K. Kim, N.H. Kim, Effects of the addition of multi-walled carbon nanotubes on the positive temperature coefficient characteristics of carbon-black-filled high-density polyethylene nanocomposites, Scr. Mater. 55 (2006) 1119.
[23] H. Xia, Q. Wang, G. Qiu, Polymer-encapsulated carbon nanotubes prepared through ultrasonically initiated in situ emulsion polymerization, Chem. Mater. 15 (2003) 3879.
[24] O.K. Park, T. Jeevananda, N.H. Kim, S.I. Kim, J.H. Lee, Effects of surface modification on the dispersion and electrical conductivity of carbon nanotube/polyaniline composites, Scr. Mater. 60 (2009) 551.
[25] O.K. Park, N.H. Kim, G.H. Yoo, K.Y. Rhee, J.H. Lee, Effects of the surface treatment on the properties of polyaniline coated carbon nanotubes/epoxy composites, Compos. Part B Eng 41 (2010) 2.
[26] S. Bhadra, D. Khastgir, N.K. Singha, J.H. Lee, Progress in preparation, processing and applications of polyaniline, Prog. Polym. Sci. 34 (2009) 783.
[27] G. Wang, Z. Shen, X. Li, C. Li, Melt processable conducting poly(aniline-co-o-anisidine)/linear low-density polyethylene composites with ethylene-acrylic acid copolymer as compatibilizer, J. Appl. Polym. Sci. 98 (2005) 1511.
[28] P. Kalappa, J.H. Lee, B.J. Rashmi, T.V. Venkatesha, K.V. Pai, W. Xing, Effect of polyaniline functionalized carbon nanotubes addition on the positive temperature coefficient behavior of carbon black/high-density polyethylene nanocomposites, IEEE Trans. Nanotechnol. 7 (2008) 223.
[29] C. Su, G. Wang, F. Huang, Y. Sun, Effect of carbon black modified with polyaniline on resistivity behavior of polyethylene/carbon black composites, J. Macro. Sci. Part B Phys. 47 (2008) 65.
[30] F. Avilés, J.V. Cauich-Rodríguez, L. Moo-Tah, A. May-Pat, R. Vargas-Coronado, Evaluation of mild acid oxidation treatments for MWNT functionalization, Carbon 47 (2009) 2970.
[31] J. Kathi, K.Y. Rhee, Surface modification of multi-walled carbon nanotubes using 3-aminopropyltriethoxysilane, J. Mater. Sci. 43 (2008) 33.
[32] J.H. Lee, K.Y. Rhee, S.J. Park, The tensile and thermal properties of modified CNT-reinforced basalt/epoxy compostes, Mater. Sci. Eng. A 527 (2010) 6838.
[33] D.S. Vicentini, G.M.O. Barra, J.R. Bertolino, A.T.N. Pires, Polyaniline/thermoplastic polyurethane blends: preparation and evaluation of electrical conductivity, J. Eur. Polym. 43 (2007) 4565.
[34] P. Hou, C. Liu, Y. Tong, S. Xu, M. Liu, H. Cheng, Purification of single-walled carbon nanotubes synthesized by the hydrogen arc-discharge method, J. Mater. Res. 16 (2001) 2526.
[35] F. Avilés, J.V. Cauich-Rodríguez, L. Moo-Tah, A. May-Pat, R. Vargas-Coronado, Evaluation of mild acid oxidation treatments for MWCNT functionalization, Carbon 47 (2009) 2970.
[36] H. Pang, Y.C. Zhang, T. Chen, B.Q. Zeng, Z.M. Li, Tunable positive temperature coefficient of resistivity in an electrically conducting polymer/graphene composite, Appl. Phys. Lett. 96 (2005) 251907.
[37] B. Pourabbas, S.J. Peighambardoust, PTC effect in HDPE filled with carbon blacks modified by Ni and Au metallic particles, J. Appl. Polym. Sci. 105 (2007) 1031.
[38] T. Kuila, S. Bose, A.K. Mishra, P. Khanra, N.H. Kim, J.H. Lee, Effect of functionalized graphene on the physical properties of linear low density polyethylene nanocomposites, Polym. Test. 31 (2012) 31.
[39] Y. Xi, H. Ishikawa, Y. Bin, M. Matsuo, Positive temperature coefficient effect of LMWPE-UHMWPE blends filled with short carbon fibers, Carbon 42 (2004) 1699.
[40] S. Wang, Z. Liang, P. Gonnet, Y.H. Liao, B. Wang, C. Zhang, Effect of nanotube functionalization on the coefficient of thermal expansion of nanocomposites, Adv. Funct. Mater. 17 (2007) 87.
[41] Y.P. Mamunya, Y.V. Muzychenko, E.V. Lebedev, G. Boiteux, G. Seytre, C. Boullanger, P. Pissi, PTC effect and structure of polymer composites based on polyethylene/polyoxymethylene blend filled with dispersed iron, Polym. Eng. Sci. 47 (2007) 34.
[42] S.P. Bao, G.D. Liang, S.C. Tjong, Positive temperature coefficient effect of polypropylene/carbon nanotube/montmorillonite hybrid nanocomposites, IEEE Trans. Nanotechnol. 8 (2009) 729.
[43] K.Y. Tsao, C.S. Tsai, C.Y. Huang, Effect of argon plasma treatment on the PTC and NTC behaviors of HDPE/carbon black/aluminum hydroxide

nanocomposites for over-voltage resistance positive temperature coefficient (PTC), Surf. Coat. Technol. 205 (2010) S279.
[44] D.W.M. Marr, M. Wartenberg, K.B. Schwartz, M.M. Agamalian, G.D. Wignall, Void morphology in polyethylene/carbon black composites, Macromolecules 30 (1997) 2120.
[45] J. Oakey, D.W.M. Marr, K.B. Schwartz, M. Wartenberg, Influence of polyethylene and carbon black morphology on void formation in conductive composite materials: a SANS study, Macromolecules 32 (1999) 5399.